Discover Energy

Research

Variability indexes for wind power

Guglielmo D'Amico[1] · **Giovanni Masala**[2] · **Filippo Petroni**[1]

Received: 10 January 2025 / Accepted: 20 May 2025
Published online: 04 June 2025

Abstract
In this paper, we propose some new measures of wind power variability based on reliability indexes. The measures are computed for continuous-time Markov models of wind power generation and for different wind parks. This allows us to compare the differences in the measurement of the variability of wind power due to the different geographical positions of the wind plants. The results have direct practical relevance and utility in the real-world wind energy sector, as they contribute to a more in-depth understanding of the variability risk of wind power generation plants.

Keywords Markov process · Rate of occurrences · Wind power

1 Introduction

Wind power is characterized by significant variability due to changing wind conditions, which can lead to both underproduction and overproduction of energy. This variability complicates the integration of wind power into energy systems and highlights the need for robust analytical frameworks to evaluate system performance under uncertain conditions. Thus, the variability of wind power generation is a key issue in the context of energy production, necessitating an ad hoc exploration of stochastic processes to effectively model and understand this challenge. The starting point involves identifying a suitable stochastic model to capture the inherent fluctuations in wind energy output. The randomness in wind power production is due to a plethora of phenomena that can have a physical nature, such as wind speed, air density, and temperature, or a technical nature, such as wake interactions and tower shadows, just to name a few of them. In this study, we focus on the role played by the wind speed process as the main determinant of the wind power. The literature is wide and ranges from continuous-time wind speed and power models based on stochastic differential equations (see, e.g., [1, 2]) to econometric ones (see, e.g., [3, 4]) and also considers multi-state models with a probabilistic structure dictated by Markov chain models (see, e.g., [5, 6]), semi-Markov chains (see, e.g., [7, 8]) and their generalizations based on indexed mechanisms (see, e.g., [9, 10]). The selection of the stochastic model of wind speed or wind power is only the first problem to be addressed. Another fundamental aspect is the identification of suitable variability measures to be evaluated. These two aspects are interrelated, as some indicators can be effectively computed for some classes of models and more difficult to calculate with others. Frequent measures of wind variability include the standard deviation, the coefficient of variation, the interquartile range, and percentile-based measures (see, e.g., [11]). More general and robust indicators were proposed in [12] with special attention to advancing the use of the robust coefficient of variation.

Guglielmo D'Amico, Giovanni Masala and Filippo Petroni have contributed equally to this work.

✉ Guglielmo D'Amico, g.damico@unich.it; Giovanni Masala, gb.masala@unica.it; Filippo Petroni, filippo.petroni@unich.it | [1]Department of Economics, University G. d'Annunzio of Chieti-Pescara, Viale Pindaro, 42, 65127 Pescara, Abruzzo, Italy. [2]Department of Economics and Business Sciences, University of Cagliari, Via Sant'Ignazio, 17, 09123 Cagliari, Sardegna, Italy.

Another stream of literature considers the loss of load hours (LoLH) as an efficiency metric of wind production. The LoLH compares the wind production with the power demand and computes the expected number of hours, within a fixed time interval, in which the power production is lower than the demand; see, e.g., [13, 14]. A detailed treatment of wind speed and power variability is given in [15] where the authors investigate 27 combinations and variations of existing methods describing the spread of wind data.

Recent studies advance wind power metrics in the frequency domain. They use the power spectral density of the wind power distribution (see, e.g., [16]). These measures do not provide information about wind power fluctuations in an interval of time and about their duration. An attempt to consider these additional features was provided by [17], where the authors proposed a conditional range metric, which is a type of wind power interval estimation over a specified time interval.

Motivated by the research of suitable variability indexes of wind power, we propose in this paper to apply some of the measures suggested in the recent paper by [18] for the reliability assessment of a multi-state system. Those measures are based on the rates of occurrence of specific events that are represented by the crossing of some thresholds by the wind power process. One of these metrics, known as the rate of occurrence of failures (ROCOF), is widely recognized. It has been extensively studied in relation to Markov processes (see [19]), semi-Markov ones (see [20]), and generalized, including different features in [21, 22]. A recent review on the ROCOF, including a description of the possible application to wind power generation, is given in [23]. Therefore, the choice of the Markov chain model is motivated by two essential reasons: the existence of a suitable model of wind speed for which it is possible to compute reliability metrics.

However, the ROCOF is not able to provide a complete description of the wind power fluctuation because it only considers the chance to move from working states to failure states at specific times. For this reason, we make use of additional measures such as the rate of occurrence of repair (ROCOR) and the ratio rate (RR). The ROCOR takes into account a system's ability to repair itself after suffering a failure; hence, it considers the chance to move from failure states to working states at specific times. The RR is the ratio of the ROCOF over the ROCOR and provides a balance between the two measures. In our framework, working states represent different levels of wind power production, while non-working (or failure) states are those in which the wind power is absent, mainly due to a too weak wind, which does not allow the turbine to produce energy, or due to a too strong wind, which imposes the shutdown of the blade to prevent structural damages.

The computation of these indicators based on a continuous-time Markov chain model of wind power is presented according to the theory developed in [18]. Next, we move on to a practical application, which concerns the production of wind energy resulting from eight locations for which we used the time series of wind speed. For some ranges of wind speed values (too low or too high), wind turbines do not produce energy, and therefore they experience a failure. We will then show the usefulness of jointly considering the indicators introduced to represent the dynamics of the system (i.e., production or not production of electricity), and we discuss the incremental information brought by the new indicators as compared to traditional ones.

The following sections are structured as follows: Section 2 describes the main reliability problem inherent in Markov processes and introduces the indicator functions and their evaluation formulas. In Section 3, we describe the dataset used for the real application, and we present the results concerning the ROCOF and ROCOR measures. Section 4 concludes with general comments.

2 Markov model and reliability indexes

We present the salient features of Markov processes in relation to the computation of reliability indicators. For more details, it is suggested to consult [24–26] and [27].

Given a continuous-time Markov process $\{X(t),\ t \in \mathbb{R}_+\}$ with a finite state space $E = \{1, 2, \ldots, s\}$, we can describe the probabilistic evolution of a system with a set of transition probability functions given $\forall i, j \in E$ by

$$P_{i,j}(t) := \mathbb{P}[X(t) = j | X(0) = i]. \tag{1}$$

These functions represent the conditional probability of visiting state j at time t under the hypothesis that the system starts from state i at time zero. Clearly, we have that $P_{i,j}(0) = \begin{cases} 1 & \text{if } i = j \\ 0 & \text{if } i \neq j \end{cases}$.

Henceforth, transition functions are assumed to have the property

$$\mathbb{P}[X(t+h) = j | X(h) = i] = \mathbb{P}[X(t) = j | X(0) = i] = P_{i,j}(t),\ \forall h > 0,$$

this is the case satisfied by time-homogeneous Markov chains.

To fully determine the dynamics of the process, we introduce the probabilities

$$\alpha_i := \mathbb{P}[X(0) = i],\ i \in E,\ \sum_{j \in E} \alpha_j = 1.$$

The vector $\boldsymbol{\alpha} = (\alpha_i; i \in E)$ is the vector of initial or starting probabilities. Moreover, we specify a set of transition rates $\mathbf{Q} = (q_{i,j})_{i,j \in E}$ with the conditions $q_{i,j} \geq 0,\ \forall i \neq j$ and $q_{i,i} = -\sum_{j \neq i} q_{i,j}$. We can interpret the elements of $\mathbf{Q}$ as:

$$q_{i,j} = \lim_{t \to 0} \frac{P_{i,j}(t)}{t},\ i \neq j, \quad q_{i,i} = \lim_{t \to 0} \frac{1 - P_{i,i}(t)}{t}.$$

The matrix $\mathbf{Q}$ of transition rates is usually called the generator matrix of the continuous-time Markov chain.

Exploiting the properties of the generator matrix and using the Chapman-Kolmogorov equation, it is possible to prove that the matrix of transition probability functions $\mathbf{P}(t) = (P_{i,j}(t))$ satisfies the following systems of differential equations (forward and backward Kolmogorov equations),

$$\dot{\mathbf{P}}(t) = \mathbf{P}(t) * \mathbf{Q} \quad \text{and} \quad \dot{\mathbf{P}}(t) = \mathbf{Q} * \mathbf{P}(t).$$

whose unique solution can be identified as follows,

$$\mathbf{P}(t) = e^{t\mathbf{Q}} := \sum_{k=0}^{\infty} \frac{\mathbf{Q}^k t^k}{k!},$$

having used the initial condition $\mathbf{P}(0) = \mathbf{I}$.

As a consequence:

$$P_{i,j}(t) = \left(e^{t\mathbf{Q}}\right)_{i,j}.$$

We deduce straightforwardly the unconditional probability that the process lies in any state j at time t:

$$p_j(t) := \mathbb{P}[X(t) = j] = \sum_{i \in E} \alpha_i P_{i,j}(t).$$

To evaluate the system performance, we exploit the transition probabilities. As a starting point, we divide the set E into two subsets: W and F. The former collects all working states in which the system is considered operational and working at different levels of performance; the latter collects all failure states in which the system is not working at different impedance conditions. We further assume that the sets W and F are nonempty and disjoint and their union gives E. We can, without loss of generality, assume:

$$W = \{1, 2, \ldots, m\},\ \text{and}\ F = \{m+1, m+2, \ldots, s\}.$$

Next, we introduce the availability and reliability functions as performability measures (see [28] for details).

We start from the block representation of the generator matrix and the initial probability vector:

$$\mathbf{Q} = \begin{pmatrix} \mathbf{Q}_{WW} & \mathbf{Q}_{WF} \\ \mathbf{Q}_{FW} & \mathbf{Q}_{FF} \end{pmatrix} \qquad \boldsymbol{\alpha} = [\boldsymbol{\alpha}_W, \boldsymbol{\alpha}_F],$$

Note that the block $\mathbf{Q}_{WW}$ contains the transition rates between couples of working states; other blocks have similar meaning, so the submatrix $\mathbf{Q}_{WF}$ contains the transition rates between the working states and the failure ones. Next $\mathbf{1}_{s,m}$ is the s-dimensional column vector whose m first elements are equal to one and the remaining $s - m$ are zero.

Now according to [28], the availability function, which gives the probability of finding the system working at time t, is:

$$A(t) := \mathbb{P}[X(t) \in W] = \boldsymbol{\alpha} * \left(e^{t\mathbf{Q}}\right) * \mathbf{1}_{s,m}. \tag{2}$$

This function quantifies the chance of finding the system working at a specific time t independently of the level of performance.

The reliability function, which gives the probability of finding the system working at any time u between zero and t, is:

$$R(t) := \mathbb{P}[X(u) \in W,\ \forall s \in [0,t]] = \boldsymbol{\alpha}_W * \left(e^{t\mathbf{Q}_{ww}}\right) * \mathbf{1}_{m,m}. \tag{3}$$

This function quantifies the probability of finding the system working over the generic time interval $(0, t]$.

The availability and reliability functions are both useful indicators that have found different extensions in the recent literature; see, e.g., [29] and the references therein. Many other reliability metrics could be evaluated in principle, such as the Mean Time to Failure (MTTF), which is defined as the average time a system or component operates before failure. Here, we depart from this direction and provide calculations for instantaneous measures, providing a description of the system behavior per unit time.

Let us now introduce some important indicators to establish the temporal performance of a system in a more detailed way. We introduce $N_f(t)$ the process that gives the number of failures up to the time t of the system. Observe that a failure consists of a transition from the set W to the set F. Hence, the ROCOF at time t is defined as

$$\text{rof}(t) := \lim_{\Delta t \to 0} \frac{\mathbb{E}[N_f(t+\Delta t) - N_f(t)]}{\Delta t}. \tag{4}$$

The ROCOF is then the time derivative of the expected number of failures up to time t. The first appearance of this concept can be found in [30] and [19]. From an operational point of view, the calculation can be performed using the following formula established in [30].

The ROCOF function of a Markov process with generator matrix $\mathbf{Q}$ and vector of initial probabilities $\boldsymbol{\alpha}$ is given by

$$\text{rof}(t) = \sum_{i \in E} \sum_{w \in W} \sum_{f \in F} \alpha_i \cdot \left(e^{t\mathbf{Q}}\right)_{i,w} \cdot q_{w,f}\,. \tag{5}$$

This indicator has a simple interpretation: if its value increases, it clearly means that the system is evolving into a state of worsening. Nonetheless, it considers only changes of states from the subset W to the subset F, as this type of transition increases the counting process $N_f(\cdot)$ in the time interval $(t, t+\Delta t)$.

Using the same logic, we can look at repair events instead of failure events. We must therefore define the counting process $N_r(t)$, representing the number of repairs by time t. According to [18], we can now define the rate of occurrence of repairs (ROCOR) at time t as:

$$\text{ror}(t) := \lim_{\Delta t \to 0} \frac{\mathbb{E}[N_r(t+\Delta t) - N_r(t)]}{\Delta t}. \tag{6}$$

The calculation rules are similar to the case of ROCOF that we can find in [30] and [19]. In fact, it is enough to exchange the role of the set of working states with that of the failure states. A simple calculation rule is given by the following equation:

$$\text{ror}(t) = \sum_{i \in E} \sum_{f \in F} \sum_{w \in W} \alpha_i \cdot \left(e^{t\mathbf{Q}}\right)_{i,f} \cdot q_{f,w}\,. \tag{7}$$

In this case, we may also provide a straightforward operational explanation for this index. For example, if the indicator rises, the system is more likely to show repairs and then exhibits a propensity to fix itself.

Finally, a third indicator was proposed in [18]. It represents an interesting mix of the first two, as it balances the tendency of the system to degrade (measured by the ROCOF) with the opposite tendency to repair (measured by the ROCOR).

It is called the ratio rate (RR) at time t and is defined by

$$\text{rr}(t) := \frac{\text{rof}(t)}{\text{ror}(t)}. \tag{8}$$

The RR indicator therefore allows us to weigh the number of failures in relation to the number of repairs in time. For example, if $\text{rr}(t) > 1$, it means that the system has a higher number of failures than repairs. Similar interpretation in the other cases.

Concerning the behavior of these indicators over time $t \to \infty$, we can take advantage of the known asymptotic behavior of Markov processes (see [31]). For example, if the Markov process is irreducible with ergodic states, it has a limiting (or steady-state) probability vector $\mathbf{L} = (L_1, \ldots, L_s)$ such that $\forall j = 1, \ldots, s$

$$L_j := \lim_{t\to\infty} P_{i,j}(t) = \frac{\pi_j / \sum_{h\neq j} q_{j,h}}{\sum_{i\in E}\left(\pi_i / \sum_{h\neq i} q_{i,h}\right)},$$

where $\boldsymbol{\pi} = (\pi_1, \ldots, \pi_s)$ is the limiting probability vector of the embedded Markov chain in the Markov process. As a consequence

$$\begin{aligned}
\mathrm{rof}(\infty) &:= \lim_{t\to\infty} \mathrm{rof}(t) = \sum_{i\in E}\sum_{w\in W}\sum_{f\in F} \alpha_i L_w \cdot q_{w,f}\,, \\
\mathrm{ror}(\infty) &:= \lim_{t\to\infty} \mathrm{ror}(t) = \sum_{i\in E}\sum_{f\in F}\sum_{w\in W} \alpha_i L_f \cdot q_{f,w}\,, \\
\mathrm{rr}(\infty) &:= \lim_{t\to\infty} \mathrm{rr}(t) = \frac{\sum_{i\in E}\sum_{f\in F}\sum_{w\in W} \alpha_i L_f \cdot q_{f,w}}{\sum_{i\in E}\sum_{w\in W}\sum_{f\in F} \alpha_i L_w \cdot q_{w,f}}\,.
\end{aligned} \tag{9}$$

3 A real data application to wind power generation

3.1 Data description

Time series of wind speeds, on an hourly basis, are from NASA's MERRA-2 project (https://gmao.gsfc.nasa.gov/reanalysis/MERRA-2). The geographical coordinates represent wind farms actually present in the area (see Fig. 1), whose coordinates are shown in Table 1.

Wind speed components are included in the MERRA-2 data set with codes U50M ("50 m east wind") and V50M ("50 m north wind"). The data range from 01/01/2005 to 31/12/2022 (157,776 records); some descriptive statistics are given in Table 2. The descriptive statistics indicate a certain variability across locations, even if all locations maintain relatively similar wind speed profiles. The mean wind speeds range from 5.39 m/s to 6.64 m/s, while the standard deviation values show significant spread, suggesting varying wind stability. Higher kurtosis values indicate more pronounced extreme wind speed events in some locations. These variations can directly impact turbine performance and reliability.

3.2 Wind speed analysis

The experimental density distribution of wind speed is shown in Fig. 2, and it has been fitted with a Weibull distribution:

$$f(v;\lambda,k) = \frac{k}{\lambda}\left(\frac{v}{\lambda}\right)^{k-1} e^{-(\frac{v}{\lambda})^k},$$

where k is the shape parameter, and λ is the scale parameter. The parameters obtained through a maximum likelihood estimation procedure are presented in Table 3. The Weibull distribution is suitable for wind speed analysis as it can accurately capture the variability observed in wind data and is widely used in wind energy studies [32].

For the purpose of this study, we assume that wind speed can be effectively represented by a continuous-time Markov process. To achieve this, we discretized the wind speed values into 11 equally spaced states in the range of $[0:22]$ m/s, with each state representing a 2 m/s interval, similar to the bin size used for the histogram in Fig. 2.

Using this discretized time series of wind speed, we estimate the transition matrix of the embedded Markov chain (Fig. 3), which shows the transition probabilities between the defined wind speed states. The transition probability matrix $\mathbf{P} = (p_{ij})_{i,j\in E}$, depicted in Fig. 4, provides a detailed representation of how the system evolves over time, capturing the probability of transitioning from one state of wind speed to another. The diagonally dominant structure suggests strong persistence in wind speed states, while the off-diagonal elements highlight probabilities of transitions to adjacent states. This reflects the natural variability of wind conditions and underscores the importance of location-specific modeling to accurately predict energy production and system reliability.

Wind turbines operate effectively only within certain wind speed ranges, which depend on their specific construction properties. For this analysis, we consider a wind turbine with a cut-in wind speed of 4 m/s, a rated wind speed of 13 m/s, and a cut-out wind speed of 20 m/s (this example is based on Nordex N117/2400, which is designed for low-wind

Fig. 1 Wind farms locations

Table 1 Wind farms coordinates

Location	Coordinates (lat., long.)
1. Medio campidano	39.5928, 8.67139
2. Buddusò	40.6743, 9.26233
3. Ulassai	39.7003, 9.51879
4. Macchiareddu	39.2030, 8.97755
5. Fiume Santo	40.8397, 8.2924
6. Campeda	40.3993, 8.79787
7. Portoscuso	39.1978, 8.43278
8. Grighine	39.9161, 8.84056

Table 2 Wind speed (m/s) statistics for each location

Location	Mean	St. dev	Skewness	Kurtosis	Min	Max
1	5.75	3.0955	0.7800	3.6356	0.01	23.38
2	5.55	3.3603	0.9838	3.9221	0.02	24.13
3	5.64	3.1829	0.8436	3.7077	0.02	24.13
4	6.25	3.3188	0.6806	3.4162	0.02	23.48
5	5.99	3.6915	0.9490	3.7051	0.01	24.60
6	5.40	2.9914	0.8532	3.6970	0.03	20.65
7	6.64	3.6796	0.7247	3.3787	0.01	24.94
8	5.39	2.9355	0.8735	3.8428	0.01	22.11

Table 3 Parameters of the Weibull distribution for wind speed series

Param./series	1	2	3	4	5	6	7	8
λ	6.49	6.25	6.35	7.05	6.74	6.09	7.49	6.09
k	1.94	1.73	1.85	1.97	1.70	1.89	1.88	1.93

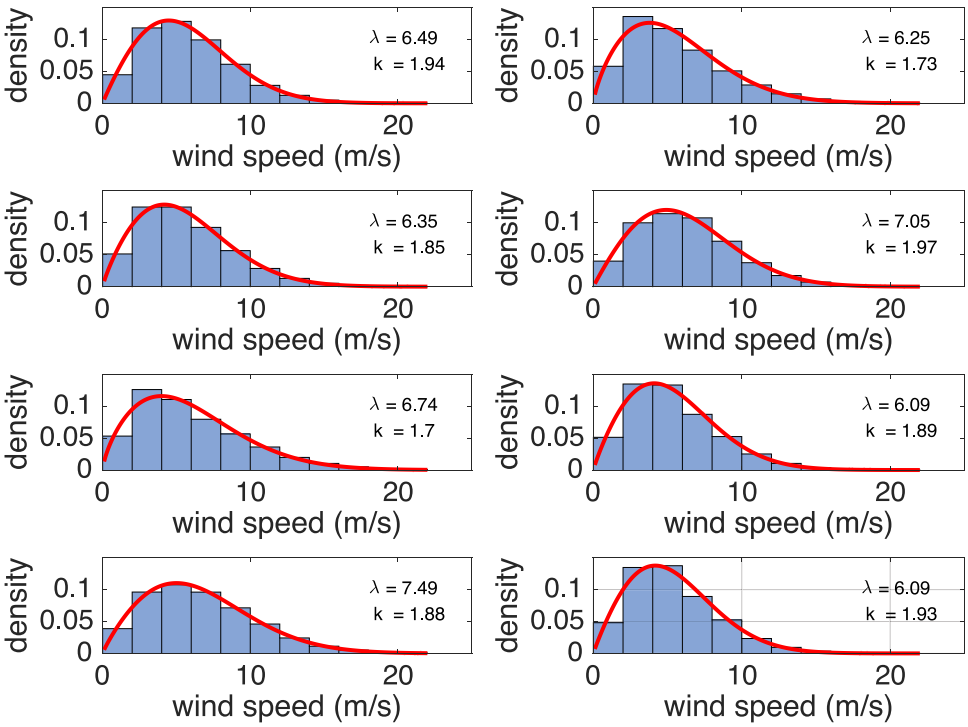

Fig. 2 Wind speed distribution fitted with a Weibull distribution

regions and has a rated power of 2.4 MW). This means that the turbine will only produce energy whenever the wind speeds fall within this range. Based on these operational limits, we divide the 11 wind speed states into two subsets: one $W = \{3, \ldots, 9\}$, which represents the working states, and two $F = \{1, 2, 10, 11\}$, which represents the failure states where no energy is produced either due to insufficient or excessive wind speed. This classification is chosen to reflect a typical commercial wind turbine that is expected to produce energy most of the time under a given wind speed distribution. It should be noted that the relationship between wind speed and wind power is not straightforward due to turbine nonlinearities, wake interactions, tower shadows, and other physical variables that affect the final power. However, in our approach, we are simply concerned with defining the thresholds that identify functioning and failure conditions; hence, we do not require an exact quantification of the power process.

Under these conditions, we applied equations (5) and (7) to estimate the Rate of Occurrence of Failures (ROCOF) and the Rate of Occurrence of Repairs (ROR) for the wind speed process. ROCOF and ROR are crucial metrics for evaluating

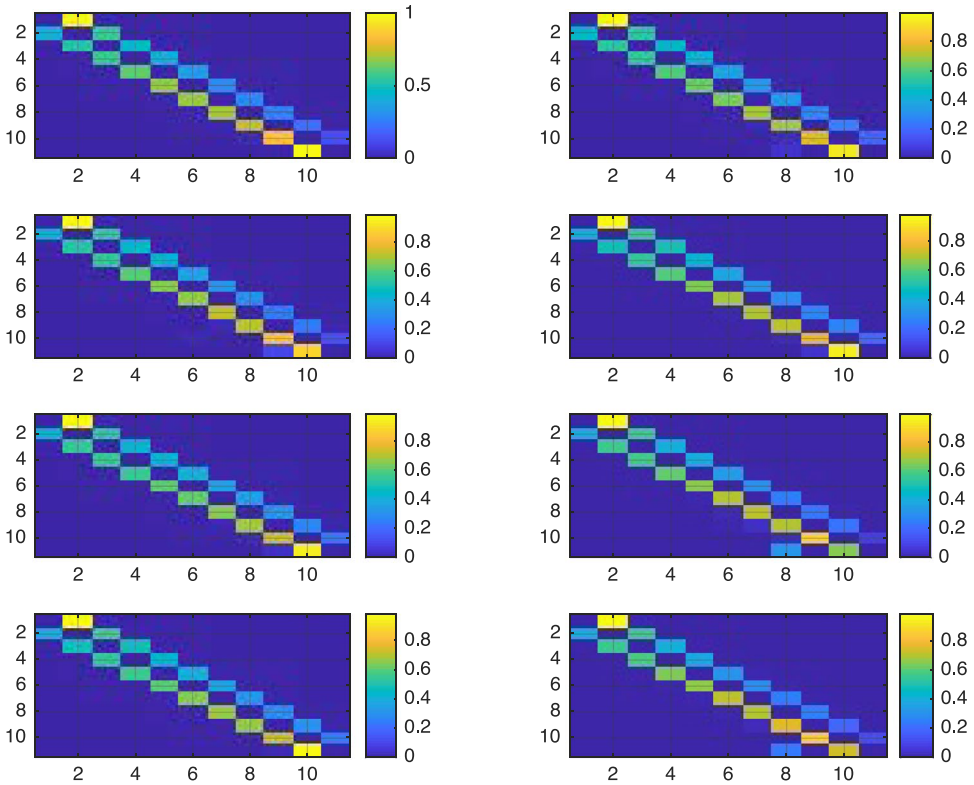

Fig. 3 Transition matrix of the embedded Markov chain

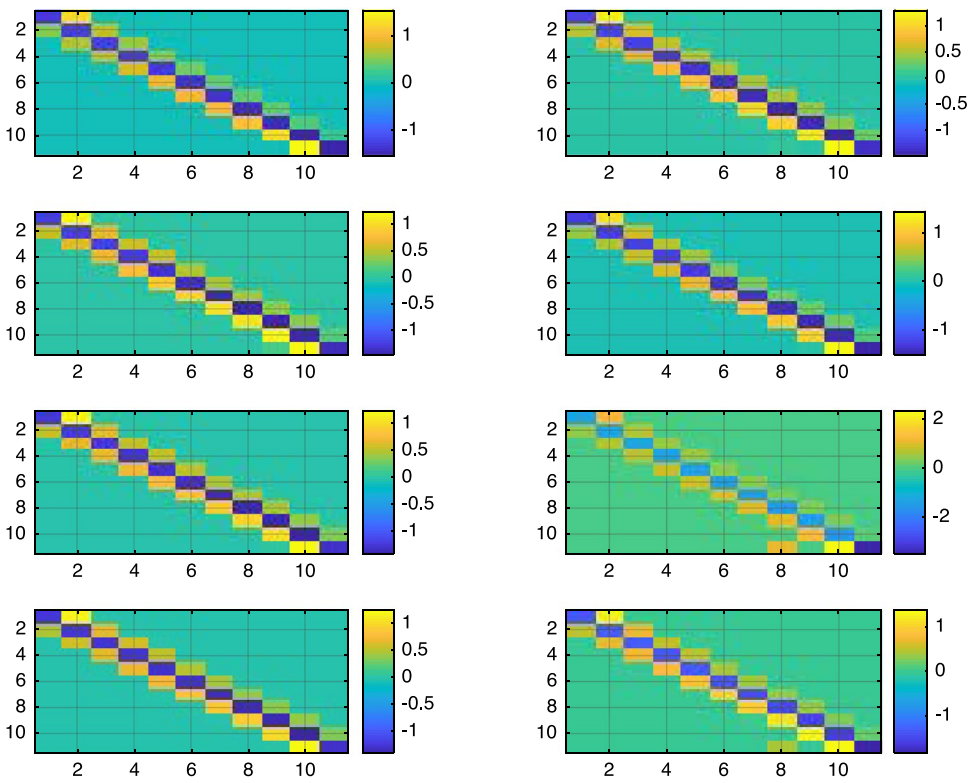

Fig. 4 Probability transition matrix of the embedded Markov chain

the reliability of wind power systems, allowing us to understand the dynamics of failure and recovery and providing valuable insights for optimizing the operational performance of wind turbines.

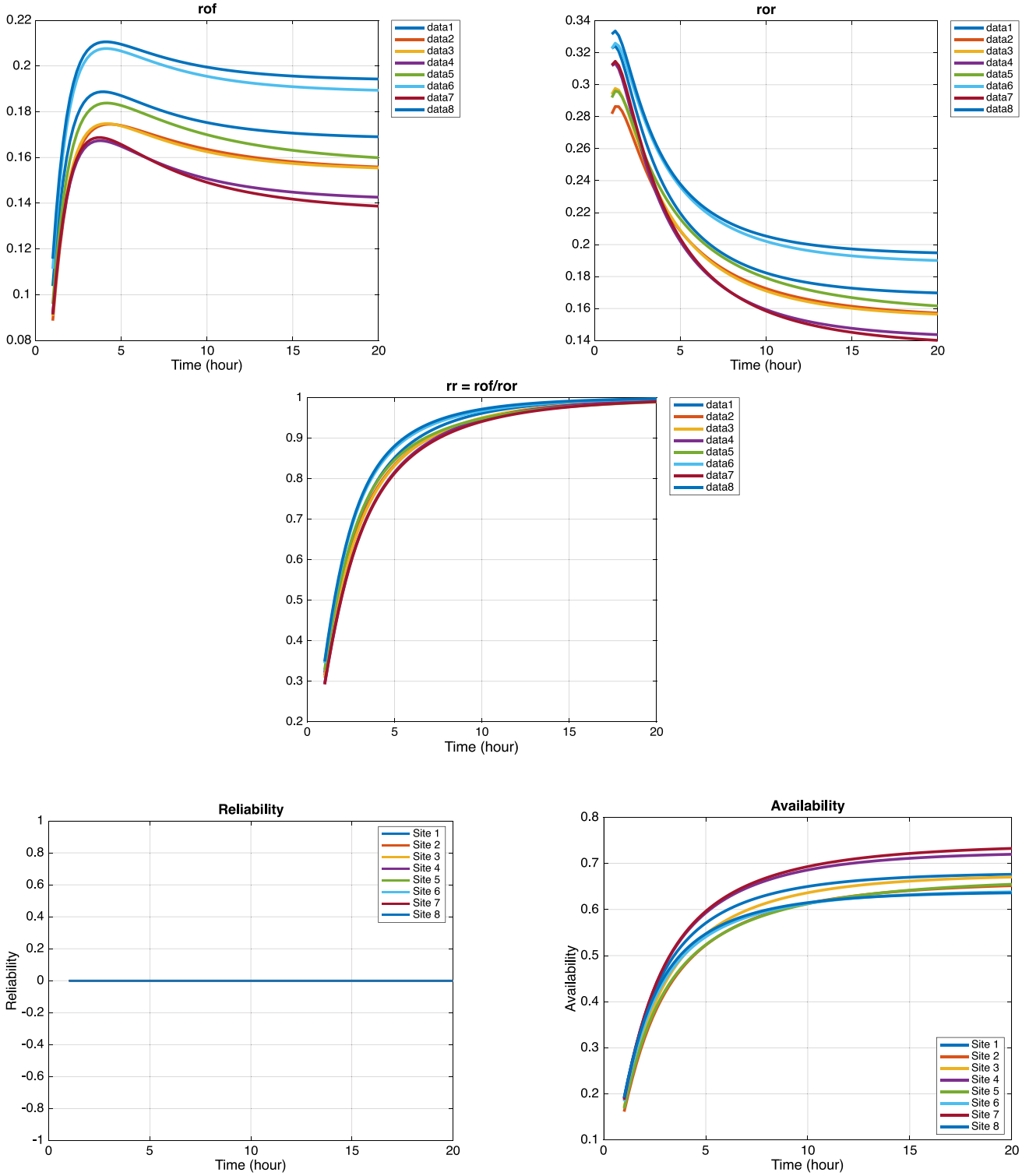

Fig. 5 ROCOF, ROR, RR, reliability, and availability for the wind speed process with initial state 1

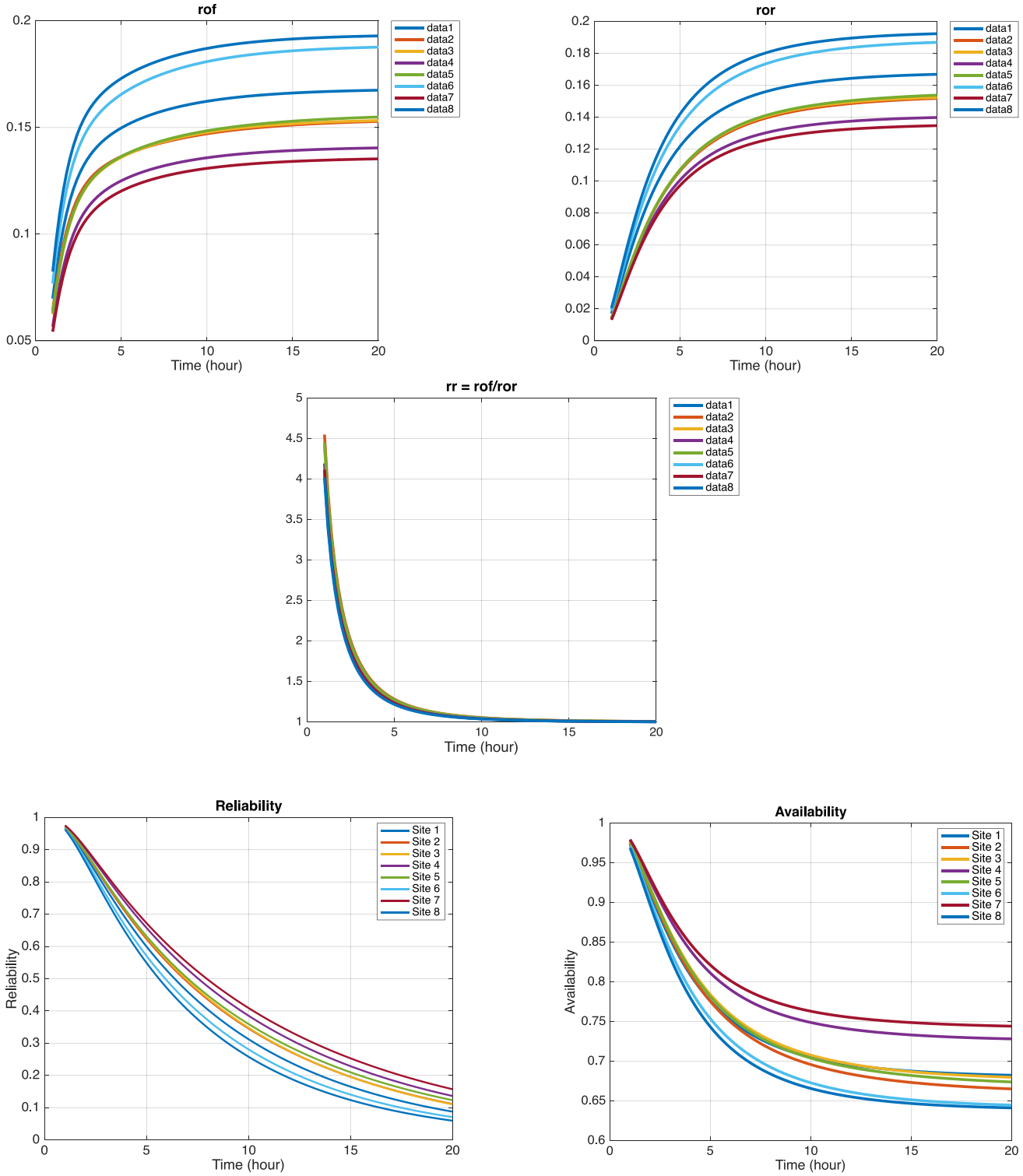

Fig. 6 ROCOF, ROR, RR, reliability, and availability for the wind speed process with initial state 5

4 Results

The results of our analysis are presented in Fig. 5, Fig. 6 and Fig. 7. Each of these figures shows the Rate of Occurrence of Failures (ROCOF), Rate of Occurrence of Repairs (ROR), and the Ratio Rate (RR) for different initial probability vectors α.

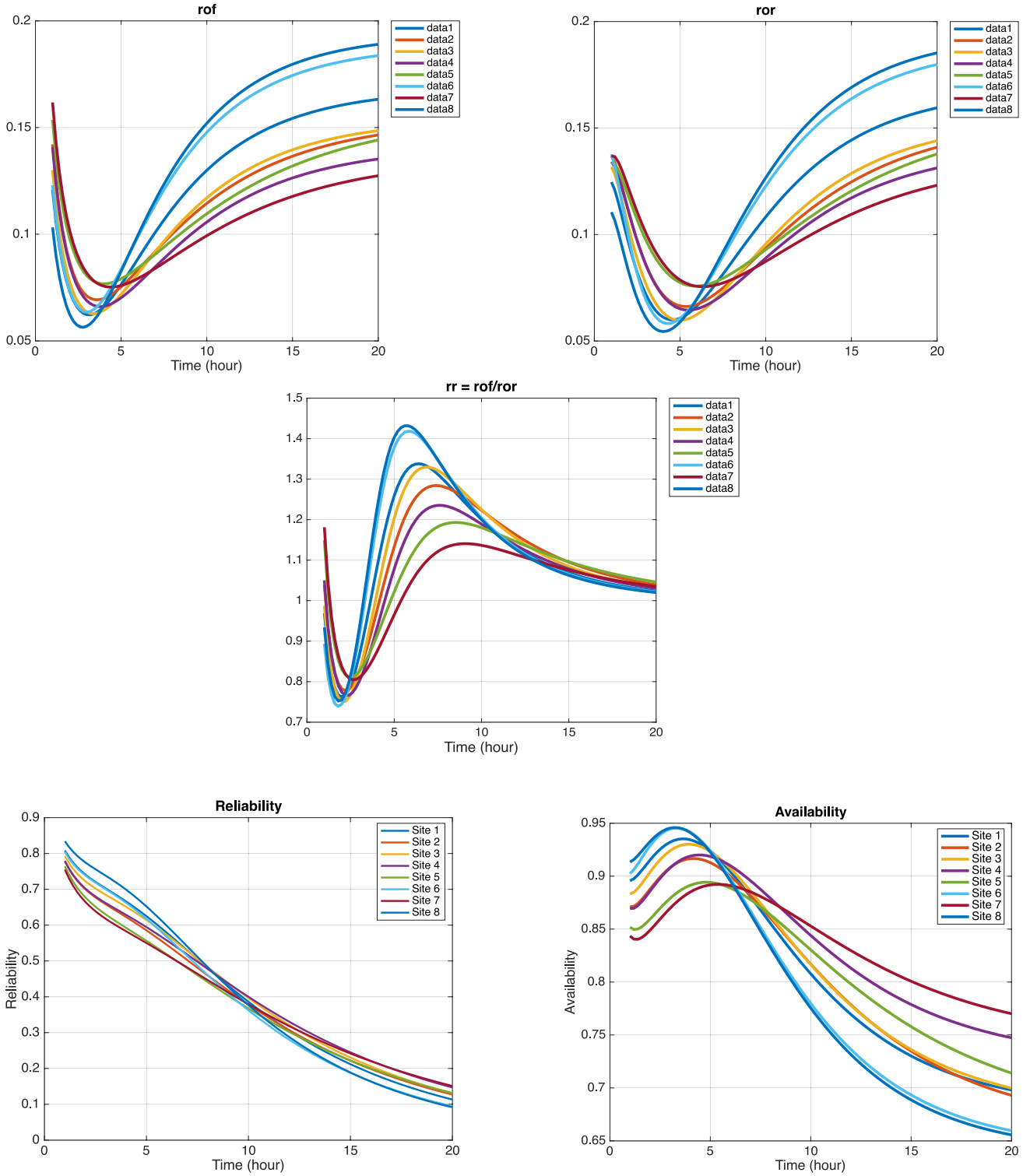

Fig. 7 ROCOF, ROR, RR, reliability, and availability for the wind speed process with initial state 9

4.1 Fig. 5: Initial wind speed state 1

Figure 5 illustrates the behavior of ROCOF, ROR, availability, and reliability for the wind speed process when the initial state is set to 1, representing a very low wind speed condition. In this scenario, we observe a divergence in the

behavior of ROCOF and ROR. Specifically, ROR starts at a relatively high value and decreases over time, while ROCOF starts at a lower value and gradually increases. This suggests that initially the system is more capable of transitioning to a working state (high ROR), but as time progresses, the repair rate decreases while the failure rate (ROCOF) increases.

The initial high value of ROR reflects the system's strong recovery capability at very low wind speeds. However, as time passes, the repair rate decreases, and failures become more prominent, as indicated by the increasing ROCOF. This dynamic leads to a convergence between ROR and ROCOF after approximately 15 h, indicating a balance between failure and repair rates.

Availability starts at zero in this case because the system is initially in a non-working state. Over time, availability increases as the system transitions to working states due to the high initial repair rate. However, as ROCOF increases and ROR decreases, availability reaches a plateau, reflecting a balance between the likelihood of transitioning into and out of the working states. Reliability, which measures the probability of staying in a working state, remains zero throughout because the system begins in a failure state and cannot achieve continuous operation from this starting condition.

Differences among sites:

- Sites 7 and 4 exhibit the highest failure rate (ROCOF) initially, resulting in slower increases in availability compared to other sites. These sites are more vulnerable to low wind conditions.
- Sites 6 and 8 show higher initial ROR values, enabling a faster recovery into working states and leading to higher availability in the early hours.
- The convergence between ROCOF and ROR happens faster for Sites 1, 3, and 5, resulting in quicker operational stability and moderate long-term availability.

This analysis highlights the transient dynamics of repair and failure rates for very low initial wind speeds. While all sites eventually reach a balance between ROCOF and ROR, the time required to achieve this and the resulting availability levels vary significantly. Sites with higher initial repair rates (e.g., 6 and 8) recover more quickly, while sites like 7 and 4 remain more vulnerable, reflecting operational challenges under low wind conditions.

4.2 Fig. 6: Initial wind speed state 5

Figure 6 presents the results obtained when the initial state of the wind speed is set to 5, which represents moderate wind speed conditions. In this scenario, the system starts at an intermediate level, which affects the transient behavior of both ROCOF and ROR. We observe that the RR ratio reaches values above 4 during the initial hours, suggesting a period where the repair rate significantly exceeds the failure rate. This indicates that, at moderate initial wind speeds, the system has a higher recovery capacity, reflected in the rapid increase in ROR compared to ROCOF.

As time progresses, the repair rate stabilizes while the failure rate gradually increases, leading to a decline in both availability and reliability. Availability begins at a relatively high value, reflecting the system's operational state at moderate wind speeds, but it decreases over time as failures accumulate and the balance between repair and failure rates shifts unfavorably. Reliability, which measures the probability of remaining continuously in a working state, also declines steadily, highlighting the inability of the system to maintain uninterrupted operation as failures become more frequent.

The transient dynamics suggest that, despite an initial advantage of high recovery rates, moderate wind speeds still present challenges in sustaining long-term operational stability. The decline in both availability and reliability underscores the need to address the effects of cumulative failures through proactive maintenance strategies.

Differences among sites:

- Sites 7 and 4 exhibit the steepest declines in availability and reliability, reflecting their lower recovery capacity and higher failure rates under moderate wind conditions.
- Sites 2 and 6 display more gradual declines, maintaining better overall performance due to their higher initial recovery capacity and more stable operational conditions.
- Site 5 shows variability in both availability and reliability during the transient phase, mirroring the pronounced fluctuations in its repair rate (ROR).

This analysis highlights that while moderate wind speeds initially offer favorable conditions for balancing repair and failure rates, the system's performance deteriorates over time as failures accumulate. Site-specific differences further emphasize the importance of tailored operational strategies to mitigate the impact of declining availability and reliability.

4.3 Fig. 7: Initial wind speed state 9

Figure 7 shows the results when the initial state is set to 9, which corresponds to a high wind speed condition. In this case, the RR ratio remains close to 1 after the initial hours, indicating a balanced relationship between failures and repairs from the beginning. The initial spike in the ROR, followed by stabilization, demonstrates that the system is initially more reactive to failures but gradually reaches a state in which both failures and repairs occur at similar rates.

Starting from a high-wind-speed state means that the wind turbines are initially in a more vulnerable condition, with a higher likelihood of experiencing failures due to high wind speeds that can push the system beyond its rated capacity. Despite this vulnerability, the system shows an ability to stabilize and achieves a balanced RR ratio over time. This indicates that turbines, even under challenging high wind conditions, manage to maintain a consistent balance between failures and repairs in the long run.

Availability initially increases as the system transitions to working states, benefiting from the initial high repair rate (ROR). However, as failures accumulate over time and the repair rate stabilizes, availability begins to decline, reflecting the system's struggle to sustain a consistent working state under high wind conditions. Reliability, which measures the probability of remaining continuously in a working state, steadily decreases throughout the period, underscoring the system's vulnerability to frequent transitions between working and failure states.

Differences among sites:

- Sites 7 and 5 exhibit higher failure rates (ROCOF) under high wind speed conditions, leading to steeper declines in availability and reliability. These sites are more susceptible to failures caused by excessive wind speeds.
- Sites 1 and 3 achieve an early balance between ROCOF and ROR, with RR values close to 1 from the beginning. This contributes to their higher availability during the initial phase and slower reliability declines, indicating greater structural resilience.
- Sites 6 and 8 show slower responses in reaching stabilization, with delayed declines in availability. However, their reliability decreases steadily, reflecting a gradual accumulation of failures over time.

This analysis highlights that high wind speeds pose significant challenges in maintaining long-term operational stability. While some sites (e.g., 1 and 3) manage to balance failures and repairs effectively, others (e.g., 7 and 5) struggle with higher failure rates, resulting in faster declines in both availability and reliability. These findings emphasize the importance of adapting maintenance and operational strategies to mitigate the impact of extreme wind conditions.

4.4 Comparison of the three scenarios

The differences observed in Figs. 5, 6, and 7 highlight the impact of varying initial wind speed conditions on the transient dynamics of wind power generation reliability. In all three cases, we see that ROCOF and ROR tend to converge over time, suggesting that, regardless of initial conditions, the system eventually reaches a state of stability. However, the rate at which this stability is achieved and the balance between failures and repairs during the transient phase can vary significantly depending on the initial wind speed state. Similarly, trends in availability and reliability add important information on how the system performs in both short-term and long-term operational contexts.

Low Initial Wind Speed (Figure 5)

At very low wind speeds, the system starts in a failure state, as indicated by zero availability and reliability. The ROR is initially high, reflecting the system's strong capacity to transition from failure to working states early on. However, as time progresses, the ROR decreases while the ROCOF increases, leading to their eventual convergence after approximately 15 h. This convergence reflects a balance between repair and failure rates, stabilizing the system.

Moderate Initial Wind Speed (Figure6)

When the system begins at a moderate wind speed, it benefits from favorable conditions for turbine operation. ROR starts high and significantly exceeds ROCOF, as shown by an RR ratio above 4 during the initial hours. This reflects the system's strong recovery capacity and resilience at moderate wind speeds. Over time, the repair rate (ROR) stabilizes, while the failure rate (ROCOF) gradually increases, leading to a decline in the RR ratio toward 1.

Availability starts at a relatively high level, indicating a high probability of being in a working state initially. However, as failures accumulate and the balance between repair and failure rates shifts, availability declines over time. Reliability exhibits a steady decrease throughout the period, reflecting the cumulative impact of failures and the challenge of maintaining continuous operation. This scenario demonstrates the system's ability to recover quickly from failures initially but also highlights the difficulty in sustaining long-term stability.

High Initial Wind Speed (Figure 7)

In the high wind speed scenario, the system begins in a more vulnerable condition, as turbines are subject to stress from excessive wind speeds. Initially, ROR, ROCOF, and RR exhibit a declining trend, reflecting a temporary reduction in both failures and repairs as the system adjusts to high wind stress. Subsequently, all three indicators rise, indicating an increase in both failure and recovery activity, eventually leading to a rebalancing of repair and failure rates.

Availability initially increases due to the high repair rate at the start, allowing the system to transition into working states. However, as failures accumulate and repair rates stabilize, availability declines, highlighting the difficulty of maintaining consistent operation under high wind conditions. Reliability, on the other hand, declines steadily throughout, reflecting the compounding effect of failures and the system's inability to sustain uninterrupted operation over time.

Overall Comparison Across Sites and Scenarios:

- Sites 7 and 5 consistently exhibit higher failure rates (ROCOF) across all scenarios, leading to steeper declines in availability and reliability. These sites demonstrate weaker resilience to varying wind conditions.
- Sites 6 and 8 show strong recovery capabilities (high ROR) but require more time to stabilize, as reflected in their delayed availability declines and gradual reliability decreases.
- Sites 1, 3, and 2 emerge as the most balanced, maintaining moderate RR ratios, slower reliability declines, and higher availability over time. These sites demonstrate superior structural resilience and operational stability.

This integrated analysis of ROCOF, ROR, RR, availability, and reliability underscores the interplay between transient dynamics and long-term performance. By considering these indicators together, operators can gain a more comprehensive understanding of site-specific challenges and opportunities, enabling the optimization of maintenance schedules and operational strategies.

5 Conclusion

In conclusion, this paper has provided an in-depth exploration of various indicators and metrics that are essential for understanding the reliability and performance of complex systems, particularly through the lens of Markov and semi-Markov processes.

Our investigation highlighted that while traditional measures, such as availability and reliability functions, offer valuable insights into system behavior over extended periods, they often fail to capture the instantaneous dynamics of system transitions. To address this gap, we introduced the Rate of Occurrence of Repairs (ROCOR) as a complementary measure to the Rate of Occurrence of Failures (ROCOF), enabling a more comprehensive evaluation of a system's capacity to recover from failures. This dual perspective not only allows for the assessment of failure likelihood, but also provides critical insights into the system's resilience, which is especially pertinent in high-variability environments like wind power generation.

The application of these concepts to wind power generation has demonstrated their practical relevance and utility in real world scenarios. By examining the transient dynamics of wind turbines under different initial wind speed conditions, we were able to illustrate how ROCOF and ROCOR evolve over time and how the initial states significantly impact system behavior. These findings are particularly relevant for optimizing maintenance strategies and improving operational reliability in renewable energy systems where variability and unpredictability pose significant challenges.

In general, this study contributes to the ongoing discourse in reliability theory by emphasizing the importance of considering both cumulative and instantaneous measures in assessing system performance. The combined use of ROCOF and ROCOR offers a richer understanding of both failure frequency and recovery capacity, ultimately providing a more balanced and actionable perspective on system reliability.

Future research could build on these findings by exploring additional applications of ROCOR in different domains, such as other renewable energy sources or industrial systems where the minimization of downtime is crucial. In addition,

investigating the effectiveness of these metrics under varying environmental and operational conditions could further enhance our understanding of system resilience and inform better decision making in reliability management. In fact, by analyzing the trend of the variability indexes, maintenance engineers can predict when it would be preferable to maintain a wind turbine according to its behavior in terms of expected failures and repairs.

Acknowledgements The authors sincerely acknowledge the reviewers for their valuable comments and suggestions, which helped to improve the quality of the manuscript.

Author contributions The authors G. D'Amico, G. Masala and F. Petroni have equally contributed to the paper.

Funding G. D'Amico and F. Petroni acknowledge financial support from the European Union - NextGenerationEU program, Missione 4 Componente 1, CUP D53D23006470006, MUR PRIN 2022 n. 2022ETEHRM "Stochastic models and techniques for the management of wind farms and power systems" by the Italian Ministero dell'Universitá e della Ricerca.

G. D'Amico and F. Petroni are members of the Gruppo Nazionale Calcolo Scientifico-Istituto Nazionale di Alta Matematica (GNCS-INdAM).

Data availability The data described in this article have been downloaded from https://gmao.gsfc.nasa.gov/reanalysis/MERRA.

Declarations

Ethics approval and consent to participate This article does not involve any research conducted on human or animal subjects.

Informed consent All individuals involved in the study gave their informed consent before participating.

Consent for publication All authors have approved the final version of the manuscript for publication.

Competing interests The authors declare no competing interests.

References

1. Zárate-Miñano R, Anghel M, Milano F. Continuous wind speed models based on stochastic differential equations. Appl Energy. 2013;104:42–9.
2. Loukatou A, Howell S, Johnson P, Duck P. Stochastic wind speed modelling for estimation of expected wind power output. Appl Energy. 2018;228:1328–40.
3. Chang W-Y, et al. A literature review of wind forecasting methods. J Power Energy Eng. 2014;2(04):161.
4. Lucheroni C, Boland J, Ragno C. Scenario generation and probabilistic forecasting analysis of spatio-temporal wind speed series with multivariate autoregressive volatility models. Appl Energy. 2019;239:1226–41.
5. Eryilmaz S, Bulanik I, Devrim Y. Computing reliability indices of a wind power system via Markov chain modelling of wind speed. Proceed Inst Mech Eng, Part O J Risk Reliab. 2024;238(1):71–8.
6. Lopes VV, Scholz T, Estanqueiro A, Novais AQ. On the use of markov chain models for the analysis of wind power time-series. In: 2012 11th International Conference on Environment and Electrical Engineering, IEEE. 2012; 770–775.
7. D'Amico G, Petroni F, Prattico F. First and second order semi-Markov chains for wind speed modeling. Physica A. 2013;392(5):1194–201.
8. D'Amico G, Petroni F, Prattico F. Performance analysis of second order semi-Markov chains: an application to wind energy production. Methodol Comput Appl Probab. 2015;17:781–94.
9. D'Amico G, Petroni F, Prattico F. Wind speed modeled as an indexed semi-Markov process. Environmetrics. 2013;24(6):367–76.
10. D'Amico G, Petroni F, Prattico F. Wind speed and energy forecasting at different time scales: a nonparametric approach. Physica A. 2014;406:59–66.
11. Jamil M, Parsa S, Majidi M. Wind power statistics and an evaluation of wind energy density. Renew Energy. 1995;6(5–6):623–8.
12. Watson S. Quantifying the variability of wind energy. Wiley Interdiscip Rev Energy Environ. 2014;3(4):330–42.
13. Casula L, D'Amico G, Masala G, Petroni F, et al. A multivariate model for hybrid wind-photovoltaic power production with energy portfolio optimization. J Energy Mark. 2022;15(3):1–29.
14. Mohiley AU, Moharil R. Selection of wind generators for optimal utilization of wind energy using reliability constraint. In: 2013 Third International Conference on Advances in Computing and Communications, IEEE. 2013; pp. 367–371.

15. Lee JC, Fields MJ, Lundquist JK. Assessing variability of wind speed: comparison and validation of 27 methodologies. Wind Energy Sci. 2018;3(2):845–68.
16. Apt J. The spectrum of power from wind turbines. J Power Sour. 2007;169(2):369–74.
17. Boutsika T, Santoso S. Quantifying short-term wind power variability using the conditional range metric. IEEE Trans Sustain Energy. 2012;3(3):369–78.
18. D'Amico G, Gismondi F, Petroni F. On some occurrence rates for Markov processes with application. In: Stochastic modeling and statistical methods. Amsterdam: Elsevier; 2025. p. 7.
19. Yeh L. The rate of occurrence of failures. J Appl Probab. 1997;34(1):234–47.
20. Ouhbi B, Limnios N. The rate of occurrence of failures for semi-Markov processes and estimation. Statist Probab Lett. 2002;59(3):245–55.
21. D'Amico G. Rate of occurrence of failures (ROCOF) of higher-order for Markov processes: analysis, inference and application to financial credit ratings. Methodol Comput Appl Probab. 2015;17:929–49.
22. D'Amico G, Petroni F. ROCOF of higher order for semi-Markov processes. Appl Math Comput. 2023;441: 127719.
23. D'Amico G, Gismondi F. Recent developments in the computation of the ROCOF of multi-state systems and its applications. Reliab Theory Appl. 2024;19:73.
24. Billinton R, Bollinger KE. Transmission system reliability evaluation using Markov processes. IEEE Trans Power Appar Syst. 1968;2:538–47.
25. Banjevic D, Jardine A. Calculation of reliability function and remaining useful life for a Markov failure time process. IMA J Manag Math. 2006;17(2):115–30.
26. Csenki A. Joint interval reliability for Markov systems with an application in transmission line reliability. Reliab Eng Syst Saf. 2007;92(6):685–96.
27. Brémaud P. Gibbs fields and monte carlo simulation. Markov Chains: Gibbs Fields, Monte Carlo Simulation, and Queues, 1999;253–322
28. Sadek A, Limnios N. Nonparametric estimation of reliability and survival function for continuous-time finite Markov processes. J Stat Plan Inference. 2005;133(1):1–21.
29. D'Amico G, Gkelsinis T. On a mixed transient-asymptotic result for the sequential interval reliability for semi-Markov chains. Mathematics. 2024;12(12):1842.
30. Ding-hua S. A new method for calculating the mean failure numbers of a repairable system during (0, t]. Acta Math Appl Sin. 1985;8(1):101–10.
31. Sobel MJ, Heyman D. Stochastic models in operations research. New York: McGraw-Hill; 1982.
32. Stevens MJM, Smulders PT. The estimation of the parameters of the weibull wind speed distribution for wind energy utilization purposes. Wind Eng. 1979;3(2):132–45.